NUKLEONIKA 2012;57(1):55–60

ORIGINAL PAPER

Collection of mobile dust in the T2R reversed field pinch

**Igor Bykov,
Henric Bergsåker,
Douglos Ogata,
Per Petersson,
Svetlana Ratynskaia**

Abstract. Intensive plasma-wall interactions in fusion devices result in the impurity production and the formation of films of redeposited material, debris and dust. In present day devices, with short pulses, the mobile dust does not pose any serious operational problems, but it is a matter of serious concern for ITER and for later power producing devices with a high duty cycle. We report results of a dust collection experiment carried out at the T2R reversed field pinch device and related heavy impurity flux measurements. Dust and impurities were collected on passive Si surface probes and on ultralow density silica aerogel collectors. The advantage of the latter method is the possibility of nondestructive capture of the micron- and submicron-sized dust particles. The toroidal and radial deposition fluxes of dust particles and impurities are estimated and discussed in the light of the dominant forces acting on the dust.

Key words: aerogel • dust • collection

I. Bykov✉, H. Bergsåker, D. Ogata, P. Petersson
Division of Fusion Plasma Physics
(Association EURATOM-VR),
KTH Royal Institute of Technology,
SE-10044 Stockholm, Sweden,
Tel.: +46 8 790 9122, Fax: +46 8 24 5431,
E-mail: igor.bykov@ee.kth.se

S. Ratynskaia
Division of Space- and Plasma Physics
(Association EURATOM-VR),
KTH Royal Institute of Technology,
SE-10044 Stockholm, Sweden

Received: 29 June 2011
Accepted: 17 February 2012

Introduction

The first speculations concerning the behavior of mobile dust particles in fusion machines were made already in the late 1970's [15]. It was soon realized that the interaction of particles with the plasma will cause melting and plasma contamination by heavy impurities. Later it was shown that the dust production rate scales with machine size and duration of the discharge [8, 20, 21], which triggered systematic studies of mechanisms responsible for dust production and transport in controlled fusion devices. Specifically, carbon and metal dust (W, Be) accumulation represents serious operational and safety concerns for the international fusion test reactor (ITER), in particular concerning tritium retention (C), explosion hazard (Be, C) and material activation by fusion neutrons (W) [9, 11, 22]. Accumulation of dust in partially hidden volumes and at hot surfaces is considered particularly harmful. Moreover, dust is a source of impurities and it had been demonstrated by modeling that dust can have a significant effect on the edge plasma profiles, transport and stability [24]. Hence detailed knowledge on dust formation and migration in fusion devices is essential.

Well developed postmortem methods may be used to obtain valuable information about the total amount of accumulated dust, dust size, its morphology and composition. It is also important to understand the dust dynamics, for two reasons. Firstly it allows to understand and predict dust mobilization and transport (cf. reviews [12, 13]); dust particles penetrating beyond the scrape-off layer (SOL) will sublimate and contribute to the main plasma impurities. Secondly, dust moving

in the SOL will collide with plasma facing components (PFC) and, depending on the impact velocity, it may contribute not only to PFC erosion and destruction but also to the dust production [13, 23].

Diagnostics of mobile dust in scrape-off layer plasmas are reviewed in [18] and include imaging with fast cameras, scattering of laser light and the recently introduced aerogel collector probe method [2, 17]. The latter technique has been known for decades in space relevant research [3, 26] and recently has been adapted for detection of dust in fusion devices [2, 14, 17–19]. The advantage of the aerogel collector method is that mobile particles can be captured and investigated in terms of size, composition and morphology, since the ultralow density collector material is capable of slowing down particles without damaging. The method allows to detect dust in the SOL even if the particles are not sufficiently hot to be incandescent, as required for example for visible imaging [18]. Finally it is possible to estimate the particle velocities from the impact tracks in the aerogel, as has been discussed in details in Refs. [2, 14, 17–19].

Due to a great mismatch between densities of Si aerogel and dust particles the latter can penetrate deep under the surface of collector. As discussed in Ref. [7], to create an impact track a particle should have initial speed above specific crushing speed, which for micron-sized metal particles is estimated to be above 100 m/s.

EXTRAP T2R is a medium-sized reversed field pinch (RFP). RFP edge conditions are different from tokamaks, with weaker magnetic field, mainly poloidal at the edge, a strongly sheared toroidal E×B drift [27] and a strongly asymmetric heat flux due to superthermal electrons [28]. Following a major rebuild in 2001, T2R is operating with a 316L stainless steel wall, protected by Mo limiters [4]. The main research with the T2R device is focused on active feedback control for suppression of MHD instabilities [5] and on the effects of imposed resonant magnetic perturbations [10]. Operation with feedback makes it possible to mitigate plasma-wall interaction, which is responsible for impurity production and likely for the generation of dust particles and droplets [1].

In the present work we report on results of dust collection experiments, using Si, and silica aerogel passive surface probes in the scrape-off layer of T2R. The aims are to further develop the aerogel dust collection method and to complement results from tokamaks, e.g. [2, 17] by providing data from an environment which is slightly different from big tokamaks, which would be useful cross-check for evaluation of the dust modeling.

Experimental setup

Figure 1 shows a poloidal cross section of the device and the position of the collector probe manipulator in the outer midplane. The minor radius and last closed flux surface at $a = 0.183$ m are defined by a poloidal array of Mo mushroom limiters. The major radius of the T2R device is $R = 1.24$ m. The vacuum vessel consists of two types of sections: bent below sections made of 316L stainless steel have inner convolution radius

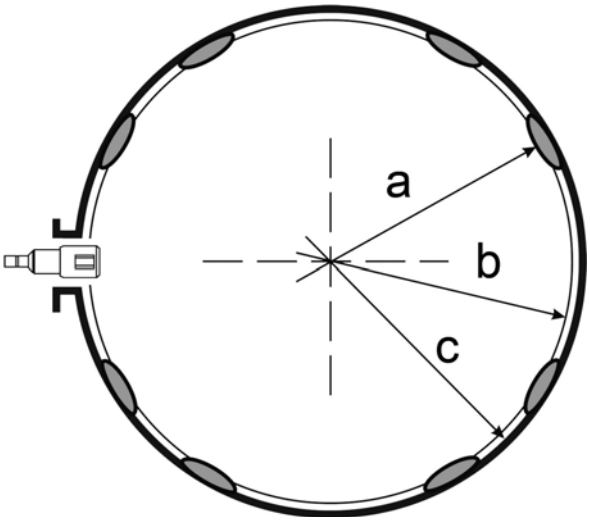

Fig. 1. Poloidal cross section at the position of probe exposure. The plasma minor radius is defined by spherically shaped protective Mo limiters. The collector probe was inserted in the outer midplane, with slit apertures open in both toroidal directions. Alternatively, samples were exposed at the wall position.

$b = 0.187$ m, whereas the port sections have inner radius $c = 0.194$ m. Si and aerogel probes were exposed in two radial positions, either sampling the toroidal fluxes in the SOL (collectors were exposed simultaneously in both toroidal directions), or sampling the radial flux at the port section wall position. The toroidal flux collectors were placed in the radial range $0.183 \text{ m} < r < 0.194$ m. To protect samples from the poloidal plasma heat flux the collectors were shielded with a boron nitride housing.

Two types of discharges were studied, either without feedback control, or with the intelligent feedback of shell type [5]. Without the feedback, the discharges were allowed to terminate spontaneously, typically at 15–20 ms. With the feedback on, the discharges can be maintained in stationary conditions for up to 100 ms, but for this work they were terminated softly at about 25 ms, in order to protect the probes from excessive heating. Representative examples of the discharges are shown in Fig. 2. As discussed in [1, 5], the discharge terminations without the feedback are abrupt and accompanied by a significant release of metal impurities (SS, Mo), whereas

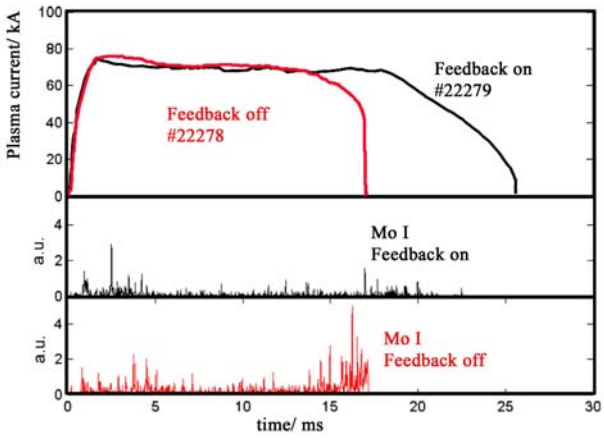

Fig. 2. Current time traces for T2R operation with and without active feedback. Also shown is the intensity of Mo I line emission during the discharge.

Table 1. Collection rates of metal (mainly SS components, Al, Mg) particles and holes on Si and spots on aerogel probes. Errors (standard deviation) due to counting statistics are indicated

Exposure direction	Cr, 10^{15} cm^{-2} · s^{-1}	Fe, 10^{15} cm^{-2} · s^{-1}	Ni, 10^{15} cm^{-2} · s^{-1}	Mo, 10^{15} cm^{-2} · s^{-1}	Total exposure, ms	Feedback
Radial, Ref. [1]	0.87	2.5	0.33	0.54	543	on
	1.1	3.8	0.49	0.76	148	off
SOL, upstream	1.7	3.8	1	1	290	on
	1.8	5.3	2.5	1.1	281	off
SOL, downstream	0.7	1.4	1	0.3	290	on
	1.8	4.3	3.6	1.8	281	off

Table 2. Time averaged deposition rates on probes exposed in upstream and downstream toroidal directions in the scrape-off layer and at the wall position

	SOL, upstream		SOL, downstream		Wall	
	FB off	FB on	FB off	FB on	FB off	FB on
Si (particles > 5 μm), cm^{-2} · s^{-1}	150 ± 40	30 ± 20	30 ± 20	90 ± 30		
Aerogel (spots > 10 μm), cm^{-2} · s^{-1}	77 ± 30	4 ± 4	11 ± 8	16 ± 8	330 ± 50	23 ± 10
Aerogel (holes < 10 μm), cm^{-2} · s^{-1}	< 1900	1590 ± 800	< 113	183 ± 80	< 300	< 280

with the feedback on (or with the gas puff termination) the termination is more gradual and without a significant release of metal. This point is illustrated here by the Mo I intensities shown in Fig. 2.

Aerogel collectors (Airglass AB, 60 kg/m^3), pure graphite surfaces and polished silicon wafers were exposed to 10–25 complete discharges, resulting in total exposure times in the range 0.25–1.3 s. To complement the measurements reported in Ref. [2], where radial dust fluxes were resolved, here a new series of aerogel exposures were performed at the SOL position to collect dust toroidally (Fig. 1). Moreover, Si probes were exposed in the discharges with similar conditions in order to measure both impurity and dust toroidal fluxes, simultaneously up- and downstream.

The following analyses of the exposed samples were performed:

(i) The areal density of the collected SS components and molybdenum on Si probes is measured by Rutherford backscattering spectrometry (RBS).

(ii) The relatively big dust particles (> 10 μm) were counted by means of optical microscopy.

(iii) The smaller particles and impact features (craters, holes) were recorded by means of scanning electron microscopy (SEM).

Compositional analysis of the captured dust was carried out by means of energy dispersive X-ray analysis (EDX).

Results of those analyses together with the known surface area and the exposure time yield the impurity and dust particle flux densities that are presented in Tables 1 and 2, respectively. These results are discussed in the following section, while below we discuss optical imaging in more detail.

To ensure that analysis of the samples takes into account only those particles collected during plasma exposure it is necessary to map their surface before and after exposure. Comparison of the relevant images allows to eliminate contribution of occasional dust present on clean samples. Such comparison is shown in Fig. 3, where

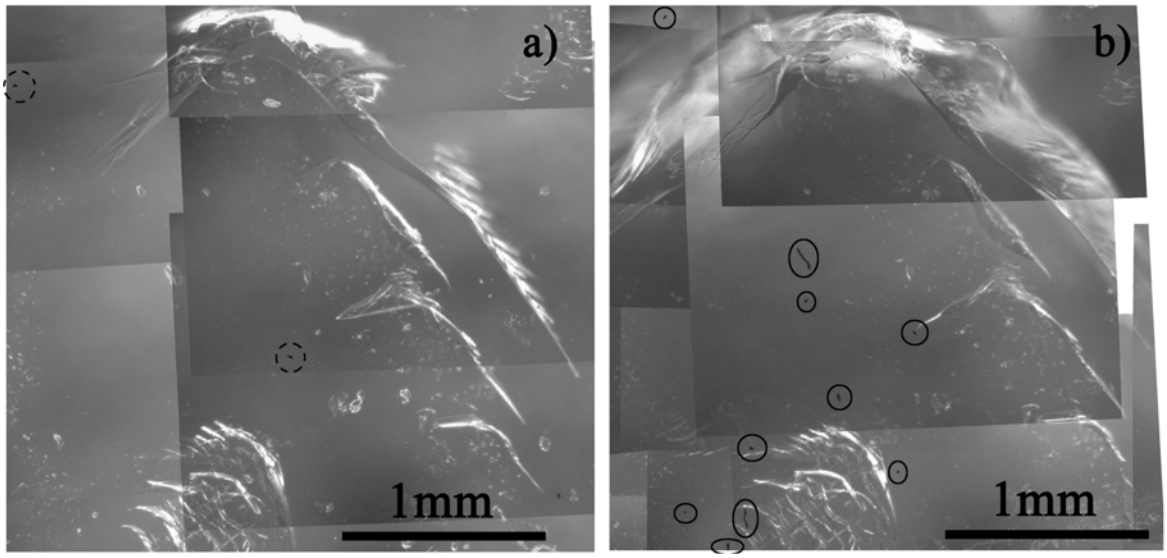

Fig. 3. a) A part of the aerogel area before the exposure. The objects indicated with dashed circles were not found at the same position after the exposure. b) The same aerogel area after the exposure. The objects indicated with solid circles were not present in the same position before the exposure. This surface was exposed at the wall position for 1091 ms of discharges with feedback mode control.

only a small fraction of the overall aerogel optical surface map is presented. It can be seen that some particles which were found at the surface before the exposure were not there anymore after the exposure, while a significant number of particles were found after the exposure, at locations where there was nothing before. Taking into account the possibility that particles present on a clean surfaces could be displaced during the exposure and counted as deposited ones, the net deposition rates are given in Table 2 with the corresponding error bars.

Results

Table 1 provides time averaged metal impurity deposition rates in discharges with and without active feedback mode control in both toroidal directions in the SOL and at the wall position measured by RBS. In addition, previously published [1] radial deposition rates are reported in the table for completeness. Hereafter up- and downstream exposure directions are given with respect to the toroidal E×B drift.

Table 2 presents collection rates of particles on both Si and aerogel surfaces. The first row of the table shows particle fluxes estimated from Si probes by SEM analysis for particles larger than 5 μm. The second row provides dust fluxes as estimated from aerogel probes by means of optical microscopy, which means that only relatively large particles (> 10 μm) are accounted for. The last row numbers are also for aerogel samples where the SEM analysis has been employed to detect small particles.

These small particles were identified via impact features of dimensions below 10 μm on the aerogel surface. To obtain representative count rates averaged over the whole exposed probe area randomly chosen points uniformly distributed over the probe surface were analyzed. EDX analysis of composition of particles collected on Si surfaces revealed that the main constituents are SS components, Al and Mg. Examples of particles caught by Si and aerogel probes under different exposure conditions are shown in Fig. 4 along with EDX signals yielded by the particles.

Discussion

As is well known [12, 13, 16, 25] charged dust particles moving in the SOL are subject to the following forces:

(i) electrostatic force,
(ii) friction force with ions and neutrals,
(iii) gravity and other forces such as recoil force during asymmetric dust ablation [13, 29], grad B force for ferromagnetic particles [16] and collisions with the wall [13, 16].

It has been shown that the friction force with ions plays major role in dust dynamics in tokamaks. This force is a function of the dust-ion relative velocity and hence ion flow profiles determine dust motion to large extent.

For the RFP configuration we anticipate the following types of ion motion to be of importance: (i) toroidal

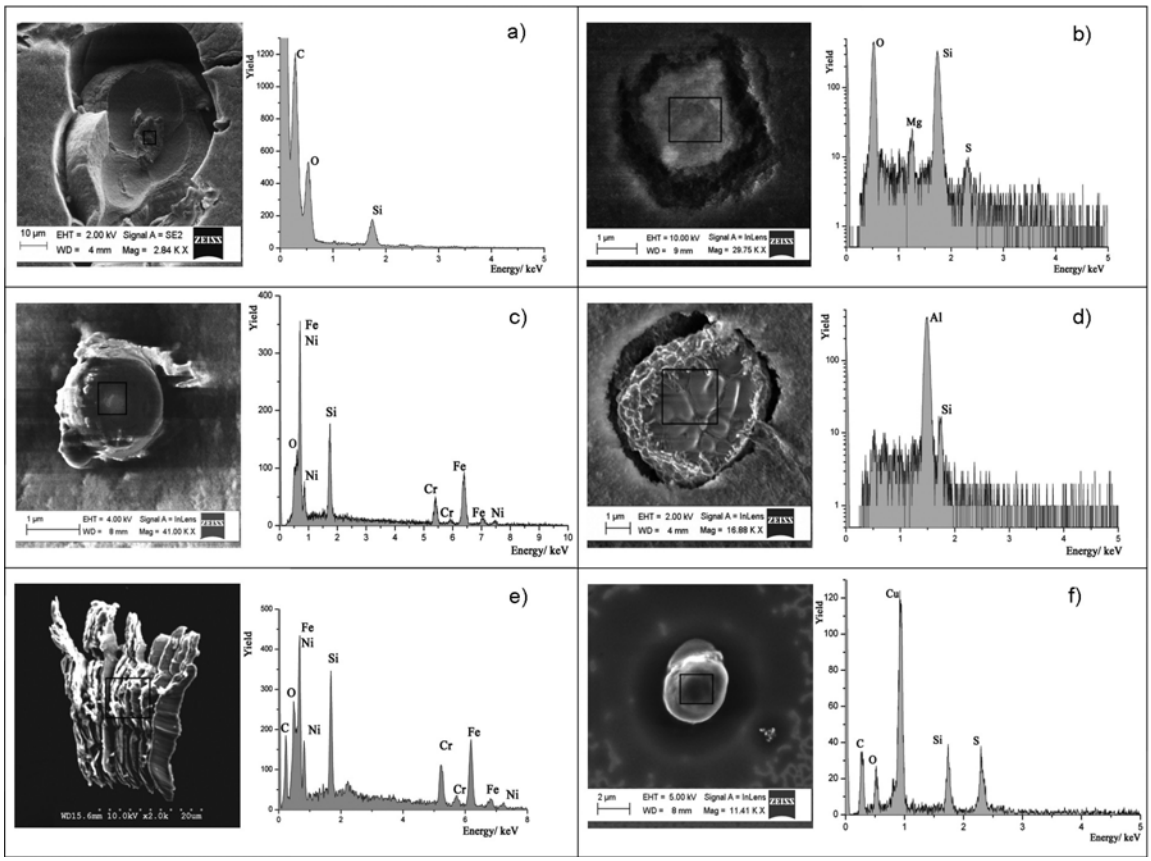

Fig. 4. SEM images of some particles, collected by aerogel (a–d) and Si (e, f) probes shown together with the corresponding EDX signal from areas marked by black rectangles. The probes were exposed to the radial flux (a), and the toroidal flux in the upstream (b, c, e), and downstream (d, f) direction.

E×B drift, which for T2R is in the range $0 < v_d < 40$ km/s for 0.172 m $< r <$ 0.194 m [27]; (ii) parallel flow along open field lines towards the limiter surfaces; (iii) ion diamagnetic drift, which in the vicinity of the probe is in the same direction as the toroidal E×B drift. Moreover a peculiarity of RFP configuration is a relatively strong radial electric field directed inwards near the wall [27], so that negatively charged dust particles are pushed out of the plasma. The results presented in Table 2 are discussed below in terms of these two forces – the ion drag and the electrostatic force.

Table 1 shows consistently higher deposition rates of metals in discharges without feedback than in discharges with intelligent shell. As discussed already in [1, 5], the high metal flux without feedback, particularly towards the end of the discharges, is associated with growing MHD mode amplitude and the slowing down of rotating modes, giving rise to more intense and more localized plasma-wall interactions. Arcing is judged likely to be one of the most important impurity production mechanisms [1]. If this is correct, mobile particles and droplets are formed in significant quantities [29]. Table 1 also shows higher deposition rates on the (E×B) upstream side than on the downstream side of the probes, which can be at least qualitatively understood as being predominantly the effect of the toroidal E×B drift of impurity ions.

Table 2 shows that at least upstream in the SOL and at the wall position the deposition rates of dust particles are likewise higher in discharges without feedback than with feedback. This finding lends some additional support to the hypothesis that arcing is a major impurity production source in T2R [1]. With feedback off, the upstream side deposition rates of particles are consistently higher than the downstream ones and the asymmetry is larger for small dust impact features than for big particles at the surface. This is qualitatively in agreement with argument that the particles are dragged toroidally by E×B ion flow. In such case the count rate for small holes shall be larger on the upstream side as indeed seen from the Table 2 for no feedback operation.

It is worth noting that there are larger numbers of big particles collected on the wall samples than upstream in the SOL. One possible explanation is that there may be a fast poloidal ion flow which provides a poloidal acceleration and throws particles out in the radial direction. Another possibility is that dust particles, ejected locally from the nearby limiters, can easily reach the collectors at the wall, while the SOL collectors are shielded from the poloidal flux.

Finally we point out that there is a finite particle flux at all collectors on the downstream side in the SOL, which contradicts the above picture of dust moving in E×B ion drift direction. Again, there are several possible explanations to the flux on the downstream side. One likely looking explanation is that the sources of particles, at the wall or at the limiters, do eject particles nearly tangentially to the wall and that they may simply be ejected with velocities in the direction opposite to the E×B flow. Indeed it is common that particles and droplets are ejected tangentially from arc spots, with velocities in the range of tens of m/s up to several hundred m/s [6]. Another possible explanation could once again be the poloidal acceleration of particles. With a strong poloidal force on the particles, it would be possible for them to reach inside the minor radius where the radial electric field changes direction (and consequently also the toroidal E×B ion drift, so that the particles could be accelerated in the opposite toroidal direction), while still being able to return to the wall, thrown out of the plasma by the centrifugal force.

Table 2 does not allow any conclusions about the relative sticking probabilities of dust particles on the two different substrates, since the size ranges are different, and the number of particles present on the silicon substrate prior to the plasma exposure was not as well characterized in SEM as with the optical mapping.

As follows from Table 1 and 2, the total Fe fluxes are generally around 4×10^{15} Fe $cm^{-2} \cdot s^{-1}$, while typical dust particle deposition rates are about 50 $cm^{-2} \cdot s^{-1}$. Supposing that the particles are typically mainly iron and that 10 μm is a representative size, the particle flux to the surfaces comes out as about 2×10^{15} Fe at. $cm^{-2} \cdot s^{-1}$, comparable to the total deposition rate of Fe.

Even though the majority (but not all) of the features observed can be qualitatively explained by taking into account only the ion drag and the electrostatic force, obviously to achieve quantitative agreement a model which accounts for all forces is necessary. Particularly, near the wall where plasma density is reduced, a delicate balance between other forces – which are negligible further away from the wall – determines the dust trajectory [16]. Moreover, the existing studies of dust dynamics in SOL [6, 12, 13, 16] show that it is sensitive to the geometry and profiles of a specific machine. Adapting the code of Ref. [16] for T2R profiles and geometry is a subject of current investigation and will be reported elsewhere.

Conclusions

Aerogel collector probes are a promising method for nondestructive dust capture in scrape-off layer plasmas [2, 17, 18]. The RFP edge plasma is different from that of big tokamaks, but dust collection experiments in T2R can be very useful for model validation and for improving the experimental technique. As this report intends to show, particle counting with aerogel collectors can be done in a reliable way. The results show that mobile particles consitute a significant impurity production channel in T2R.

References

1. Bergsåker H, Menmuir S, Rachlew E, Brunsell PR, Frassinetti L, Drake JR (2008) Metal impurity fluxes and plasma-surface interactions in EXTRAP T2R. J Phys Conf Ser 100:062030
2. Bergsåker H, Ratynskaia S, Litnovsky A, Ogata D, Sahle W (2011) Studies of mobile dust in scrape-off layer plasmas using silica aerogel collectors. J Nucl Mater 415;S1:S1089–S1093
3. Brownlee DE, Horz F, Newburn RL *et al.* (2004) Surface of young jupiter family comet 81P/Wild 2: View form the stardust spacecraft. Science 304:1764–1769
4. Brunsell PR, Bergsåker H, Cecconello M *et al.* (2001) Initial result from the rebuilt EXTRAP T2R RFP device. Plasma Phys Control Fusion 43:1457 (doi:10.1088/0741-3335/43/11/303)

5. Brunsell PR, Kuldkepp M, Menmuir S *et al*. (2006) Reversed field pinch operation with intelligent shell feedback control in EXTRAP T2R. Nucl Fusion 46:904–913
6. De Temmerman G, Bacharis M, Dowling J, Lisgo S (2010) Dust creation and transport in MAST. Nucl Fusion 50:105012
7. Domínguez G, Westphal AJ, Jones SM, Phillips MLF (2004) Energy loss and impact cratering in aerogels: theory and experiment. Icarus 172:613–624
8. Federici G, Andrew P, Barabaschi P *et al*. (2003) Key ITER plasma edge and plasma-material interaction issues. J Nucl Mater 313–316:11–22
9. Federici G, Skinner CH, Brooks JN *et al*. (2001) Plasma--material interactions in current tokamaks and their implications for next step fusion reactors. Nucl Fusion 41:1967 (doi: 10.1088/0029-5515/41/12/218)
10. Frassinetti L, Olofsson KEJ, Brunsell PR, Drake JR (2011) Implementation of advanced feedback control algorithms for controlled resonant magnetic perturbation physics studies on EXTRAP T2R. Nucl Fusion 51:063018
11. Girard J-Ph, Garin P, Taylor N, Uzan-Elbez J, Rodriguez--Rodrigo L, Gulden W (2007) ITER, safety and licensing. Fusion Eng Des 82:506–510
12. Krasheninnikov SI, Pigarov AYu, Smirnov RD *et al*. (2008) Recent progress in understanding the behavior of dust in fusion devices. Plasma Phys Control Fusion 50;12:124054
13. Krasheninnikov SI, Pigarov AYu, Smirnov RD, Soboleva TK (2010) Theoretical aspects of dust in fusion devices. Contrib Plasma Phys 50;3/4:410–425
14. Morfill G, Räth C, Li Y-F *et al*. (2009) Dust capture experiment in HT-7. New J Phys 11:113041
15. Ohkawa T (1977) Dust particles as a possible source of impurities in tokamaks. Kaku Yugo Kenkyu 37:117–131
16. Proverbio I, Lazzaro E, Ratynskaia S *et al*. (2011) The dynamics of ferromagnetic dust particles in the FTU tokamak. Plasma Phys Control Fusion 53:115013
17. Ratynskaia S, Bergsåker H, Emmoth B, Litnovsky A, Kreter A, Phillips V (2009) Capture by aerogel – characterization of mobile dust in tokamak scrape-off layer plasmas. Nucl Fusion 49:122001
18. Ratynskaia S, Castaldo C, Bergsåker H, Rudakov D (2011) Diagnostics of mobile dust in scrape-off layer plasmas. Plasma Phys Control Fusion 53:074009
19. Ratynskaia S, Castaldo C, Giovannozzi E *et al*. (2008) *In situ* dust detection in fusion devices. Plasma Phys Control Fusion 50;12:124046
20. Rubel M, Cecconello M, Malmberg JA *et al*. (2001) Dust particles in controlled fusion devices: morphology, obsevations in the plasma and influence on the plasma perfirmance. Nucl Fusion 41:1087–1099
21. Sharpe JP, Petti DA, Bartels HW (2002) A review of dust in fusion devices: Implications for safety and operational performance. Fusion Eng Des 63/64:153–163
22. Shimomura Y (2007) ITER and plasma surface interaction issues in a fusion reactor. J Nucl Mater 363/365:467–475
23. Smirnov RD, Krasheninnikov SI, Pigarov AYu, Benson DJ, Rosenberg M, Mendis DA (2009) Modeling of velocity distributions of dust in tokamak edge plasmas and dust-wall collisions. J Nucl Mater 390/391:84–87
24. Smirnov RD, Krasheninnikov SI, Pigarov AYu, Roquemore AL, Mansfield DK, Nichols J (2011) Modeling of dust impact on tokamak edge plasmas. J Nucl Mater 415;S1:S1067–S1072
25. Smirnov RD, Pigarov AYy, Rosenberg M, Krasheninnikov SI, Mendis DA (2007) Modelling of dynamics and transport of carbon dust particles in tokamaks. Plasma Phys Control Fusion 49:347–371
26. Tsou P (1995) Silica aerogel captures cosmic dust intact. J Non-Cryst Solids 186:415–427
27. Vianello N, Spolaore M, Serianni G, Bergsåker H, Antoni V, Drake JR (2002) Properties of the edge plasma in the rebuilt Extrap-T2R reversed field pinch experiment. Plasma Phys Control Fusion 44:2513–2523
28. Welander A, Bergsåker H (1998) Measurements of hot electrons in the Extrap T1 reversed-field pinch. Plasma Phys Control Fusion 40:319 (doi:10.1088/0741--3335/40/2/011)
29. Wolff H (1991) Arcing in magnetic fusion devices. Nucl Fusion Suppl 1:97–107